Unsteady Loading of Horizontal Axis Wind Turbines by Atmospheric Turbulence.

J. Michael Graham[1] , Kevin Gouder[1] and Ian A. Milne[2]
[1]Department of Aeronautics, Imperial College London, London, UK
[2]Oceans Graduate School, University of Western Australia, Perth, Australia.
E-mail: grahamjmr@aol.com

1 INTRODUCTION.

Horizontal Axis Wind Turbines (HAWTs) have continued to increase in size to provide economies of scale and the fluctuating loads resulting from interaction with Atmospheric Boundary Layer (ABL) turbulence have become increasingly challenging. Rotors normally operate at high tip-speed ratio $\Lambda(=\Omega R/U_\infty)$, Ω being the rotor speed, R its radius and U_∞ the free stream wind speed at hub height. The unsteady blade loading is dependent on both the mean shear and, since $\Lambda >> 1$, on the streamwise component of the turbulence velocity. Loading calculations are normally either performed stochastically, or increasingly, in the time domain using synthesised time histories and blade element theory assuming mean flow response subject to the rotor blocking effect but the response to turbulence without this modification. However, distortion (ie. stretching and rotation) of the incident turbulence vorticity by the mean upstream flow field of the rotor can, as for other structures in an ABL, significantly intensify the approaching streamwise component of fluctuating velocity and increase its correlation across the rotor disc. Both effects raise the levels of unsteady loading of the rotor. In contrast the blocking potential flow opposing the streamwise component of turbulence lowers turbulence intensity as it does the mean velocity. Recent full-scale field tests have measured turbulence in the induction zone of HAWT rotors using Lidar. The low frequency turbulence (large eddies), was found to be modified significantly in wind flows [1, 2, 3] and tidal flows [4]. Depending strongly on the ratio of the correlation length-scale of the turbulence to rotor diameter and on the below- or above-rated operational condition distortion/ blocking of the flow can amplify or attenuate the unsteady loads. Information on ABL turbulence intensities and length-scales [5] are available for making assessments. When the turbulence length-scale is small compared to the rotor diameter the distortion process satisfies the conditions for Rapid Distortion Theory (RDT) [6] and this theory has been used [7] to compute the turbulence incident on a rotor for a range of rotor resistance. The actuator disc theory for HAWT rotors also applies to porous discs which are often used to simulate turbines and compared with the rotor in the present work.

2 EXPERIMENT

.

2.1 Rotor and Disc Models

A three bladed, 0.5m diameter model rotor was designed to give a near uniform resistance across the rotor disc with wake induction factor $a_0 \approx 1/3$, the optimum power value. Two porous discs laser cut from board, with diameters 0.45m and 0.245m and open area ratios 0.555 and 0.529 respectively to give flow resistance similar to the rotor disc, were tested for comparison. The rotor was operated at a tip-speed ratio of 4.0 giving chord Reynolds 6400 at ¾ radius in a mean wind of 10m/s at 0.375m hub height. Both rotor and porous discs were mounted on short shafts attached to a load cell (Nano17 and Gamma130-10 types being used) and the mean and fluctuating axial forces sampled at 10kHz. The rotor was controlled by a Magtrol torque-RPM sensor and controller to rotate at 1500RPM. The geometric blockage ratio of the models in the working section was 4.3%, 3.5% and 1.0% respectively. No blockage corrections were applied.

DOI 10.5258/WES/P0014

2.2 Simulated ABL and Turbulence Intensities.

The working section of the Imperial College large closed-loop wind tunnel is 3m wide by 1.5m high by 20m long. A 1:400 scale simulation of an ABL with a surface roughness length of 0.01m was generated by a standard set-up [5] using upstream Counihan spires and a fence followed by 15m of development over a roughened floor. Velocity measurements were made using Dantec hot-wire anemometer probes. The mean velocity and streamwise turbulence intensity at the test position are shown in figure 1. The integral correlation length $R_{11}(x)$ at hub height was evaluated from the measured frequency spectrum to be 0.41m assuming Taylor's hypothesis.
These tests were supplemented by tests of the rotor and porous discs in homogeneous turbulence 12 mesh-lengths downstream of a 0.125m square mesh turbulence grid.
At this station the turbulence length-scale was 0.030m with RMS intensity 0.61m/s for a mean wind speed of 10.0m/s. These tests were to evaluate the effect of much smaller turbulence length-scale to rotor diameter ratios.

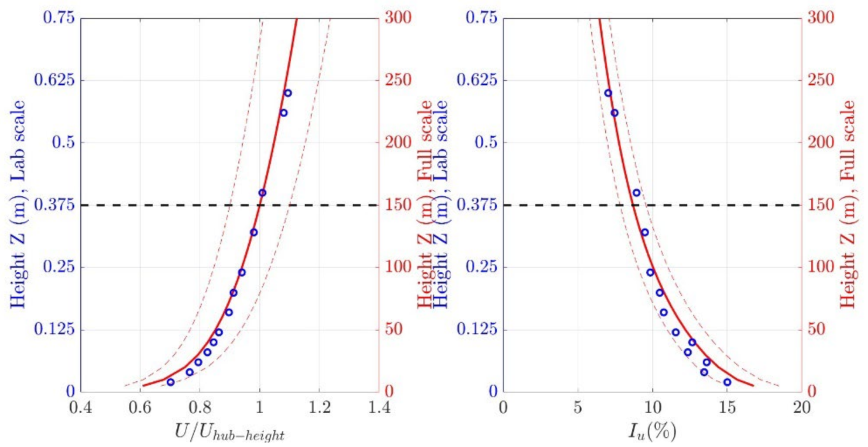

Figure 1 Wind Tunnel Simulated ABL profiles (a) $U(z)/U_{hub}$, (b) $\sqrt{\langle u^2 \rangle}/U_{hub}$

2.3 Spectra and Correlations of the Turbulence.

The grid turbulence was found to conform closely to the empirical von-Karman spectrum function $\Phi_{11\infty}$, spectra $S_{11\infty}$ and 2-point correlations $R_{11\infty}$ for quasi-isotropic turbulence [8]:

$$\Phi_{11\infty}^{VK}(\kappa_\infty) = \frac{1}{4\pi U_\infty}\left(1.339 L_{x\infty}\tau_\infty^*/\kappa_\infty^{*2}\right)^2 \frac{C\overline{u^2}_\infty \kappa_\infty^{*4}}{(1+\kappa_\infty^{*2})^{\frac{17}{6}}}$$

$$S_{11\infty}(\kappa_{1\infty}) = \frac{4L_{x\infty}\overline{u^2}_\infty}{U_\infty\left(1+\kappa_{1\infty}^{*2}\right)^{5/6}}.$$

$$R_{11}(\Delta r^*) = \frac{1}{\Gamma(1/3)}\left(\frac{\Delta r^*}{2}\right)^{1/3}\left\{K_{1/3}(\Delta r^*) - \Delta r^* K_{2/3}(\Delta r^*)\right\},$$

Here κ_1 is streamwise wavenumber, $\tau^2 = \kappa_2^2 + \kappa_3^2$ and $\boldsymbol{\kappa}^2 = \kappa_1^2 + \tau^2$. $K_{1/3}$, $K_{2/3}$ are Bessel functions and * indicates non-dimensionalisation of wavenumber (κ_j^*) and transverse separation (Δr^*).

However for the ABL turbulence it was found, as has been observed by others, that the transverse horizontal correlation coefficient $R_{11\infty}(\Delta y^*)$ had a much more pronounced negative loop than the vertical coefficient $R_{11\infty}(\Delta y^*)$, figure 2a. This could be better represented, as shown in the figure, by a modified expression for the correlation derived from the empirical spectrum function with an additional term added to that function. With $\eta_0 = 2$ giving the best fit this changes the streamwise wave-number (or frequency) spectrum by a small amount, as shown in figure 2b, to:

DOI 10.5258/WES/P0014

$$S_{11\infty}(\kappa_{1\infty}) = \frac{81 - 15\eta_0/(1 + \kappa_{1\infty}^{*2}}{81 - 6\eta_0} S_{11\infty}^{VK}(\kappa_{1\infty})$$

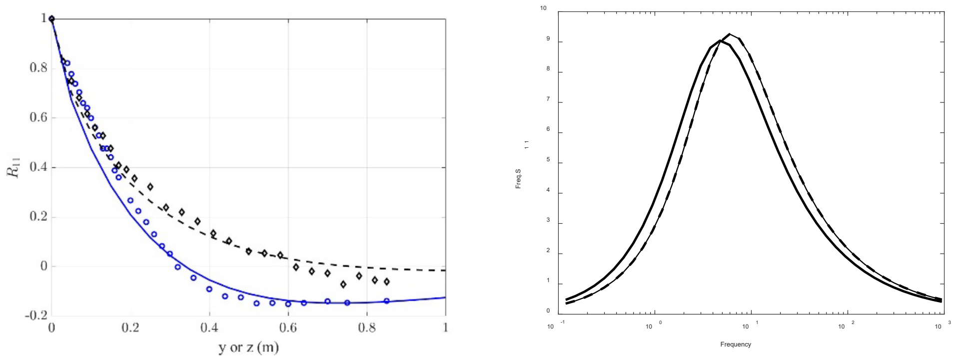

Figure 2(a) measured vertical (♦) and horizontal (o) correlation R_{11} compared with modified empirical formulae. (b) Unmodified (-) and modified (---) von Karman frequency spectrum S_{11}. .

2.4. Distorted turbulence in the induction zone.

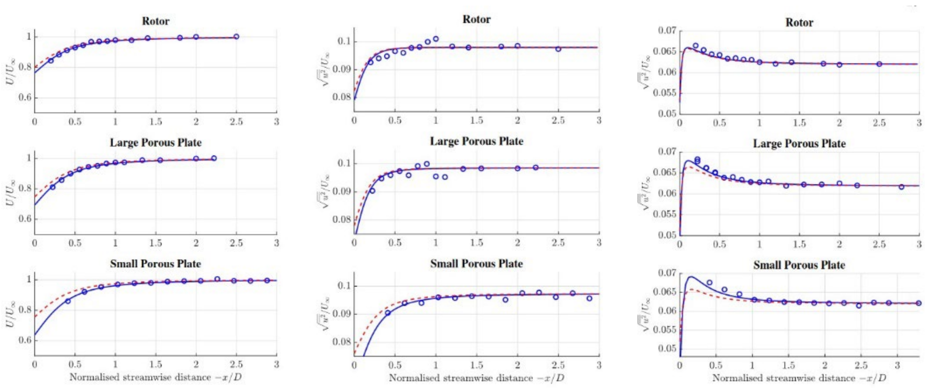

Figure 3(a) Mean flow, (b) u_{RMS} intensity of ABL turbulence, (c) grid turbulence in the induction zone.

Measurements of mean velocity and streamwise turbulence intensity along the upstream axis of each model are compared in figure 3 (a) with mean flow actuator disc theory and in (b) and (c) with distortion theory interpolated for turbulence length-scale to disc diameter ratio between quasi-steady conditions [2] causing no distortion for large scale ratios and large intensification given by RDT [7] for small scales. Distortion occurs over an upstream distance which scales on the body diameter (the scale of the mean flow causing the distortion). The intensities are also affected progressively by blocking potential flow due to disc resistance [9] opposing the streamwise turbulence velocity over a distance which scales on the turbulence length-scale. It is noticeable that the rise in intensity due to distortion is only obvious for the small length-scale grid turbulence, being too small to be seen against the overwhelming blocking reduction effect in the ABL cases.

2.5 Axial force spectra

The time dependent axial force on each disc depends linearly on the instantaneous streamwise velocity of the turbulence incident at the plane of the disc after distortion. It is calculated similarly as for the above blocking effect to which it is related, by interpolating between quasi-steady theory and the potential blocking theory [9] as described above. The prominent peaks at ~ 20Hz and 25Hz are due to structural resonance and rotation frequency blade-shear interaction. Considering that these are log-linear spectra the agreement of the computed results with the measured data is good.

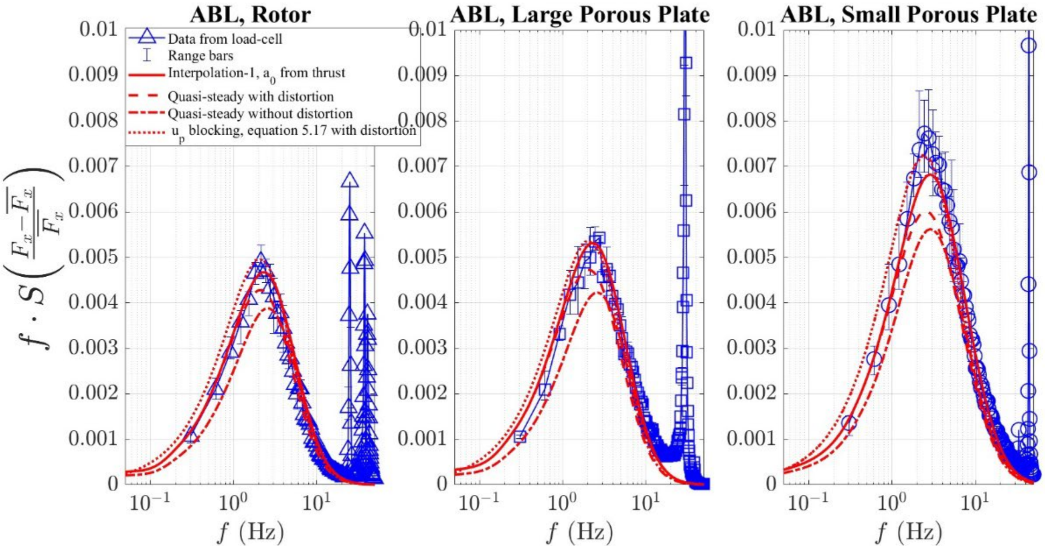

*Figure 4 Measured: frequency.PSD of Rotor Axial Force, ABL turbulence, (a) Rotor, (b) Large Porous Plate, (c) Small Porous Plate. Theoretical predictions: (— , ---, -.-., **….**).*

3. CONCLUSIONS

Induction zone turbulence intensities and axial forces induced by them on a model rotor and two porous discs in a simulated turbulent ABL has been measured and shown to compare well with interpolated formulae which combine quasi-steady theory with small length-scale RDT and a potential back-flow due to blocking. The turbulence in the ABL, unaffected by the discs, has also been studied and a modified empirical spectrum suggested to give a better fit to the horizontal transverse correlation coefficient $R_{11\infty}(\Delta y^*)$.

4. REFERENCES

[1] Pena A., Mann J. and Dimitrov N. (2017) "Turbulence characteristics from a forward facing nacelle Lidar", *Wind Energy Sci*., **2**, 133.

[2] Mann J., Pena A., Troldborg N.J, and Anderson S. (2018) "How does turbulence change approaching a rotor?", *Wind Energy Sci.,* **3**, 293.

[3] Chamorro L. P. (2015) "Turbulence effects on a full-scale 2.5MW horizontal axis wind turbine under neutrally-stratified conditions", *Wind Energy* **18**, 339.

[4] Milne I.A. and Graham J.M.R. (2019) "Turbulence velocity spectra and intensities in the inflow of a turbine rotor", *Jnl. Fluid Mech*. **870**, R3.

[5] ESDU (2002) "Strong winds in the ABL", Rep. **82026** & **85020** IHS Inc, London.

[6] Batchelor G.K. and Proudman I. (1954) "The effect of rapid distortion of a fluid in turbulent motion" , *Quart. Jnl. Mech. App. Math.,* **7,** 83.

[7] Graham J.M.R. (2017) "Rapid distortion of turbulence into an open turbine rotor" *Jnl. Fluid Mech.* **825**, 764.

[8] Deaves D.M. and Harris R.I. (1978) "A mathematical model of the structure of strong winds" *Construction Industry Research and Information Association*, Tech Rep.**76**.

[9] Batchelor G.K. (1960) "Theory of Homogeneous Turbulence", *Cam. Univ. Press.*, **ch.4**, 58.

DOI 10.5258/WES/P0014